Chemosphere xxx (xxxx) xxx

Contents lists available at ScienceDirect

Chemosphere

journal homepage: www.elsevier.com/locate/chemosphere

Clarifying the *in-situ* cytotoxic potential of electronic waste plastics

Pujiang Shi [a], Yan Wan [a], Agnès Grandjean [b], Jong-Min Lee [a, c], Chor Yong Tay [a, d, e, *]

[a] Energy Research Institute, Nanyang Technological University, 1 Cleantech Loop, 637141, Singapore
[b] CEA, DES, ISEC, DMRC, Univ Montpellier, Marcoule, France
[c] School of Chemical and Biomedical Engineering, Nanyang Technological University, 62 Nanyang Dr, 637459, Singapore
[d] School of Materials Science and Engineering, Nanyang Technological University, 50 Nanyang Avenue, 639798, Singapore
[e] School of Biological Sciences, Nanyang Technological University, 60 Nanyang Dr, 637551, Singapore

HIGHLIGHTS

- Metal concentrations in 8 discarded electronic waste plastics (E-plastics) exceeded safety standards.
- No observable acute toxicity in 6 different E-plastics exposed human cell lines.
- Leaching of toxic elements from E-plastics is negligible in biological milieu.
- Quantitative assessment of toxic elements is inadequate to forecast E-plastics toxicity.

GRAPHICAL ABSTRACT

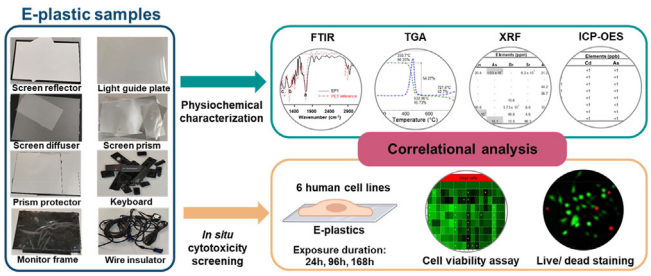

ARTICLE INFO

Article history:
Received 11 August 2020
Received in revised form
13 October 2020
Accepted 20 October 2020
Available online xxx

Handling Editor: Grzegorz Lisak

Keywords:
Electronic wastes
Plastics
Hazardous materials
Toxicity
Public health

ABSTRACT

Plastics in waste electronics (E-plastics) account for approximately 20% of the entire global electronic waste (E-waste) stream. Most of the E-plastics are not recycled as the presence of toxic additives (e.g. heavy metals, brominated flame retardants (BFRs), antimony, etc.) have associated environmental and health concerns. However, the majority of the studies are focused on quantitative assessment of the toxic constituents in E-plastics, while empirical information regarding the potential toxic effects in humans is largely lacking. To gain a deeper appreciation into the toxicological profile of E-plastics, *in situ* time-dependent exposures of 6 different human cell lines to a panel of 8 representative E-plastics recovered from liquid crystal displays (LCD), keyboards, screen frames, and wire insulators were conducted. Although several hazardous elements (e.g. Pb, As, Sb, Zn, Cu, etc) were detected at concentrations that far exceed the limit values permitted by the Restriction of Hazardous Substances Directive and EU Directives in the panel E-plastics, in-depth analysis of the 144 unique cell viability data points and live-dead staining experiments suggest that the acute and sub-chronic toxic effects of E-plastics in direct contact with human cells are negligible. These observations agreed with the inductively coupled plasma-optical emission spectrometry data, which revealed that leaching of these toxic additives into the biological milieu is not sufficiently high to trigger a cytotoxic response up to a continuous culture period of 2 weeks. The novel insights gained from this study are posited to further clarify the uncertainty associated with the safety and circular economy implementation of E-plastics.

* Corresponding author. Energy Research Institute, Nanyang Technological University, 1 Cleantech Loop, 637141, Singapore.
E-mail address: cytay@ntu.edu.sg (C.Y. Tay).

https://doi.org/10.1016/j.chemosphere.2020.128719
0045-6535/

1. Introduction

Electronic waste (E-waste) is one of the fastest-growing solid waste streams globally. In 2016, the total amount of E-waste was an astonishing 44.7 million metric tons (Sahajwalla and Gaikwad, 2018; Vanessa Forti et al., 2020). By the year 2030, this number is expected to increase to 74.7 million metric tons at an annual growth rate of ~3–4% (Vanessa Forti, 2020). Despite the rapid increase in E-waste generation, only about 15% was collected and recycled, with the majority of the E-waste being disposed-off largely in landfills or incinerated (Sahajwalla and Gaikwad, 2018). Among the many types of materials that are found in E-waste, electronic waste plastics (E-plastics) constitute a significant portion and are approximated to account for up to 20% of total E-waste by volume (Ma et al., 2016). Specifically, the production of E-plastic increased by around 20% to 10.72 million metric tons in 2019 compared to 2014, and this number is expected to reach a staggering 14.94 million metric tons by 2030 (Vanessa Forti, 2020). While significant progress has been made to reclaim valuable metals from E-wastes such as spent batteries (Rarotra et al., 2020; Wu et al., 2020) and printed circuit boards (PCB) (Qiu et al., 2020, 2021), efforts to recycle post-consumer E-plastics is generally lagging. In reality, plastics used in electronic products such as electrical wire insulator, keyboards, and monitors are typically made of recyclable polymers such as acrylonitrile butadiene styrene (ABS), polyvinyl chloride (PVC), polyethylene terephthalate (PET), polystyrene (PS), poly (methyl methacrylate) (PMMA), and polyurethane (PU). (Vanessa Forti, 2020). However, it is also well-established that E-plastics are often tainted with a myriad of toxic flame retardants, heavy metals, plasticizers, pigments, and modifiers additives, which have been identified as potential environmental and health hazards, which hamper recycling (Hahladakis et al., 2018).

E-plastics have been documented to contain numerous toxic chemicals such as lead (Pb), arsenic (As), antimony (Sb), copper (Cu), barium (Ba), and brominated flame retardants (BFRs) (Senthil Kumar and Baskar, 2015). These additives may or may not be chemically bound to the polymer matrix. Additionally, electrical heating may also potentially contaminate the E-plastics as a result of the migration of heavy metals or additives from the metallic components (e.g. pins, printed circuit board, etc.) to the plastics (Vimala et al., 2009; Hahladakis et al., 2018; Mao et al., 2020). Lead (Pb) is a highly potent systemic toxicant that can affect almost every organ, importantly, the neurotoxic actions of lead (Pb) such as cellular apoptosis, excitotoxicity, and impairment to neurotransmission processes, especially in the developing brain, are widely documented (Mishra, 2009; Wani et al., 2015). Arsenic (As) is a protoplastic poison since it affects primarily the sulphydryl group of cells causing malfunctioning of cell respiration, cell enzymes, and mitosis (Sarkar and Paul, 2016). Exposure to antimony (Sb) concentrations above 9 mg/m^3 will result in eye, skin, and lung irritation, while chronic exposure will potentiate lung, heart, and gastrointestinal diseases (Denys et al., 2009). Although copper is required for the proper functioning of many important enzyme systems, the acute lethal dose of Cu (II) for adults lies between 4 and 400 ppm (per body weight), and excessive copper ions can cause symptoms typical of food poisoning (headache, nausea, vomiting, diarrhea) at subtoxic doses (Jantsch et al., 1984; Cavallo et al., 2002). Solubilized barium (Ba) salts can cause muscle poisoning, leading to significant hypokalemia, secondary respiratory paralysis, and malignant arrhythmia, resulting in serious consequences (Ananda et al., 2013). There are currently more than 75 types of BFRs (Eriksson et al., 2001). Some BFRs are unstable under thermal stress and may turn to extremely toxic polybrominated dioxins and furans (PBDD/F) during thermal processing (Weber and Kuch, 2003; Schlummer et al., 2007). BFRs such as polybrominated diphenyl ethers (PBDEs), tetrabromobisphenol A (TBBPA), and polybrominated biphenyls (PBBs) found in E-plastics can perturb the production of thyroid hormone, interfere with estrogenic and androgen pathways (Hallgren and Darnerud, 2002; Hamers et al., 2006), induce hyperactivity (Branchi et al., 2002), cause cognitive impairment (Eriksson et al., 2001; Dufault et al., 2005), resulting in dose-dependent spatial learning and memory deficits (Yan et al., 2012).

Given its potential adverse public health impacts, examining the toxic effects of E-plastics is therefore fundamental to the safe implementation of a new plastic circular economy (CE) model. The presence of these toxic chemicals and additives may disrupt the CE and directly affect the recyclability and reuse of E-plastics. For instance, compared with outdoor levels of toxic metals (e.g. lead, chromium, zinc, etc.), E-waste recycling activities have been associated to several-fold higher production of heavy metal enriched total suspended particles (TSP) that far exceeds the World Health Organization (WHO) levels (Song and Li, 2014; Hahladakis et al., 2018). Besides workplace exposure to these toxic additives, electronic goods consumers are not spared either. In an earlier study, several heavy metals such as lead (Pb), cadmium (Cd), nickel (Ni), and silver (Ag) have been detected in the plastic housing of mobile phones at levels that may be harmful to the environment and human health (Nnorom and Osibanjo, 2009). Application of the USEtox® life cycle impact assessment (LICA) model has shown that Hg, Cr, Pb, Sb, and Br found in mobile phone plastics present considerable ecotoxicity and health (cancerous and non-cancerous) risks (Singh et al., 2020). Furthermore, a recent study reported that among the more than 600 black non-electronic consumer plastics tested, bromine (Br) was detected in almost 50% of samples with concentration ranging from 1.5 to 133,000 ppm, while lead (Pb) and antimony (As) were found in ~25% of the black plastics (Turner, 2018). These findings suggest that the contamination and the inadvertent exposure of the E-plastics associated additives in our daily life are more pervasive than expected (Turner, 2018). While these findings have raised significant public health concerns, it should be emphasized that the adverse health effects associated with the E-plastics are mostly inferred based on the quantitative assessment of the harmful additives they contain. Our current understanding of the actual toxic potential of the E-plastics is inadequate and remains far from being complete.

Herein, to better appreciate the potentially toxic effects of E-plastics, an unbiased *in situ* toxicity assessment of 8 representative E-plastics collected from a local recycling plant (Virogreen Pte Ltd, Singapore) was conducted. The panel E-plastics was selected, in part, based on their relative abundance in the E-waste stream (Buekens and Yang, 2014) (Vanessa Forti, 2020). The E-plastics was first thoroughly characterized to determine its physicochemical constituents using Fourier-transform infrared spectroscopy (FTIR), thermogravimetric analysis (TGA), and X-ray fluorescence analyzer (XRF). Thereafter, to accurately examine the potential cytotoxicity of the E-plastics, the test materials were placed in intimate contact (ISO 10993–5, 2009; MHLW, 2012) with a panel of 6 different primary and immortalized human cell lines from tissues that are representative of the different potential routes of exposure such as skin contact and ingestion. With our *in vitro* experimental approach, any direct (cell-materials interaction) or indirect (cell-leachable interaction) biological damages inflicted by the E-plastics under physiological conditions are posited to be evident. Baseline acute and sub-chronic cytotoxicity information was determined using the PrestoBlue assay to measure cell metabolism and live/dead staining to examine cell viability. This study provides the first (to the best of our knowledge) comprehensive evaluation of E-plastic toxicity using a variety of human cell lines.

2. Materials and methods

2.1. Sample collection and preparation

Representative E-plastics were curated from Virogreen (Singapore) Pte. Ltd. The E-plastics consisted of scraps from computers, liquid-crystal display (LCD), laptops, keyboards, various phones (mobile and landline), electrical insulators, and personal digital assistants (PDAs), etc. The samples were transported to the laboratory and manually dismantled by screwdrivers and penknives, and the printed circuit board, metallic and glass parts were carefully removed. The plastic components were cut into a square shape (12 × 12 mm) by a mechanical puncher, washed thoroughly with double distilled water, air-dried, and inventoried accordingly. For *in vitro* cytotoxicity studies, the samples were sterilized in 70% ethanol for 3 times (15 min each time), followed by a washing step using Phosphate Buffer Saline (PBS).

2.2. Fourier transform infrared spectroscopy (FTIR)

FTIR spectra of various E-plastics were obtained using an FTIR spectrometer (PerkinElmer Frontier, Ohio, United States). The E-plastics were manually cut using penknives, and the samples were grounded into fine powder manually by a mortar and pestle. Then, the obtained powder was mixed with KBr powder and compacted into a pellet for the FTIR examination. The spectra were investigated in the wavenumber range of 400–4000 cm^{-1}. The obtained FTIR spectra were input in KnowItAll IR Spectral Library (Bio-Rad Laboratories, Hercules, California, United States) to identify each type of E-plastics.

2.3. Thermal gravimetric analysis (TGA)

The thermal stability of the different E-plastics was analyzed by thermal gravimetric analysis (TGA, Q500, TA Instruments, New Castle, United States). Changes to the sample weight were measured over a temperature range of 25 °C to 900 °C (20 °C/min) in a nitrogen atmosphere. Derivative thermogravimetric analysis (DTG) was used to determine the decomposition temperature of the E-plastics.

2.4. X-ray fluorescent analyzer (XRF)

The E-plastics samples (12 × 12 mm) were prepared according to published protocols (Riise et al., 2000; Chaqmaqchee et al., 2017). Elemental analysis was carried out using a modified handheld X-ray fluorescence analyzer (Vanta C Series Handheld XRF analyzer, Olympus, Tokyo, Japan). The handheld XRF analyzer was pre-calibrated by the manufacturer for plastic analysis. For safety reasons, the XRF analyzer was stabilized by a field stand during measurements, and the plastic samples were put on a silicon drift detector within a protective shield. Exposure duration of approximately 180–500 s was used for each analysis, including a dwell time of 60 s in the low energy range (30 kV and 66.67 μA: Cl, Cr, and Ti) and main energy range (50 kV and 40 μA: all remaining elements). The generated X-rays spectra were automatically deconvoluted and semi-quantified to determine the dry weight elemental concentrations (parts per million, ppm).

2.5. Cell lines and culture

Human keratinocyte (HaCaT), human dermal fibroblasts (HDF), human gastric adenocarcinoma cell line (MKN), human colon cell lines (SW480), human bone osteosarcoma cells (MG63) and ASC52telo, hTERT immortalized adipose-derived mesenchymal stem cells (ADSCs, SCRC-4000) were purchased from American Type Culture Collection (ATCC). ADSCs were maintained in mesenchymal stem cell basal medium with the addition of a mesenchymal stem cell growth kit (PCS-500-030 and PCS-500-040). The other cell lines were maintained in Dulbecco's Modified Eagle Medium (DMEM, Sigma-Aldrich) with the addition of 10% Fetal Bovine Serum (Gibco) and 1% Penicillin/Streptomycin.

2.6. Cell viability assay

To ensure fair comparisons, cells were seeded onto each type of E-plastics (12 × 12 mm) at a fixed seeding density of 5×10^4 cells/E-plastics. PrestoBlue reagent (Thermal Fisher) was used to evaluate the cell viability at day 1, 4, and 7 respectively as per the earlier report (Wang et al.). Briefly, 1 ml of DMEM cell culture media containing 10% PrestoBlue and 5% FBS was incubated with each sample respectively, then 200 μl of each sample was aspirated into 96 well plates, their absorbance values at 570 and 600 nm were tested by a microplate reader (Molecular Devices SpectraMax M2). Cells cultured on normal tissue culture plastics (TCP) were served as controls. Subsequently, the cell viability was calculated according to the following formula:

$$\%Cell\ viability = \frac{Prestoblue\ reduction\ of\ cells\ on\ E-plastics}{Prestoblue\ reduction\ of\ cells\ on\ TCP} X100\%$$

2.7. Live/dead assay

Samples at day 1 and 7 were incubated with fluorescein diacetate (FDA, 8 μg/ml) and propidium iodide (PI, 20 μg/ml) in phosphate-buffered saline (PBS) for 5 min. Thereafter, the samples were observed under a fluorescence microscope (Carl Zeiss), the live (FDA, excitation: 495 nm and Emission: 517 nm) and dead cells (PI, excitation: 538 nm and Emission: 617 nm) were shown in green and red colors respectively. The exposure time was automatically optimized by the imaging software. The fluorescent images of live (green) and dead (red) cells were further analyzed by ImageJ. Briefly, the images were first converted into an 8-bit format and background signals were removed by adjusting the threshold. Thereafter, the integrated intensities of the live and dead cells in the images were measured.

2.8. Inductively coupled plasma-optical emission spectrometry (ICP-OES)

To determine the concentration of leached heavy metals, the E-plastics were fully submerged in the cell culture media (i.e. ADSCs growth medium and DMEM) in 50 ml tubes at an equivalent weight ratio of plastics to cell culture media as per the cell viability tests. The tubes were securely sealed and placed in an oven at 37 °C for 7 days. Thereafter, the culture media (10 ml) was collected and sampled using the inductively coupled plasma-optical emission spectrometry (ICP-OES, Agilent Technologies, California, United States) as reported earlier (Wu et al., 2020).

2.9. Statistical analysis

All data were expressed as mean ± the standard deviation. Statistical analysis was performed by pairwise comparison of

experimental categories using a two-tailed, unpaired Student's t-test and multiple comparisons using single-factor analysis of variance (ANOVA) and post hoc Tukey tests, using SPSS Statistics version 22.0. A *p*-value of less than 0.05 is considered statistically significant.

3. Results and discussion

3.1. FTIR polymer identification of E-waste plastics

End-of-life personal computers and mobile devices are the fastest growing waste streams in modern society. In terms of volume, the E-plastics derived from electrical wire insulator, keyboards, and monitors are among the highest (Vanessa Forti 2020). Accordingly, we have selected 8 different representative discarded E-plastic samples. They were labeled as EP1 to EP8 as shown in Fig. S1. EP1 (reflector film) is a white and flexible plastic sheet. EP2 (light guide plate) is a highly transparent plastic sheet that guides light from light-emitting diode (LED) to the whole display area. EP3 (screen diffuser) is presented as a whitish and stretchable plastic thin film. EP4 (screen prism) is a moderate flexible plastic sheet, with highly aligned grooves on it. EP5 (prism protector) is a translucent flexible plastic sheet that confers scratch resistance properties to the LCD. EP6, EP7, and EP8 are keyboard, screen frame, and wire insulator, respectively. Throughout the paper, we would use the abbreviated terminology to refer to the respective E-plastics.

Not all the E-plastics were labeled with standardizing resin codes. Therefore, FTIR spectroscopy was employed to determine the chemical identities of the various E-plastics. Chemical characteristics of the E-plastics could be differentiated by detecting the well-established chemical functionalities-specific infrared absorption bands (1450-4000 cm^{-1}) and fingerprint region (400-1450 cm^{-1}) (Al-Oweini and El-Rassy, 2009; Al-Ali and Kassab-Bashi, 2015; Dzulkurnain et al., 2015; Li et al., 2017; Jung et al., 2018). Fig. 1 shows the FTIR spectra of the various E-plastic samples. To determine the polymer types, the sample-specific absorption peaks were identified based on published data (Table 1) and the FTIR spectra were matched using the KnowItAll IR Spectral Library. The best-matched reference FTIR spectra (red dash-dot line) are overlapped in the respective graphs. Accordingly, we were able to determine the polymer types for the respective E-plastics as such: EP1 – PET; EP2 – PMMA; EP3 – acrylic and methacrylic polymers; EP4 – glass-reinforced PET; PEP5 – PMMA, EP6 – ABS, EP7 – acrylic polymers, and EP8 – PVC.

3.2. XRF determination of toxic content in E-plastics

XRF spectroscopy is a non-destructive and effective method to detect and identify hazardous heavy metals in the E-plastics with

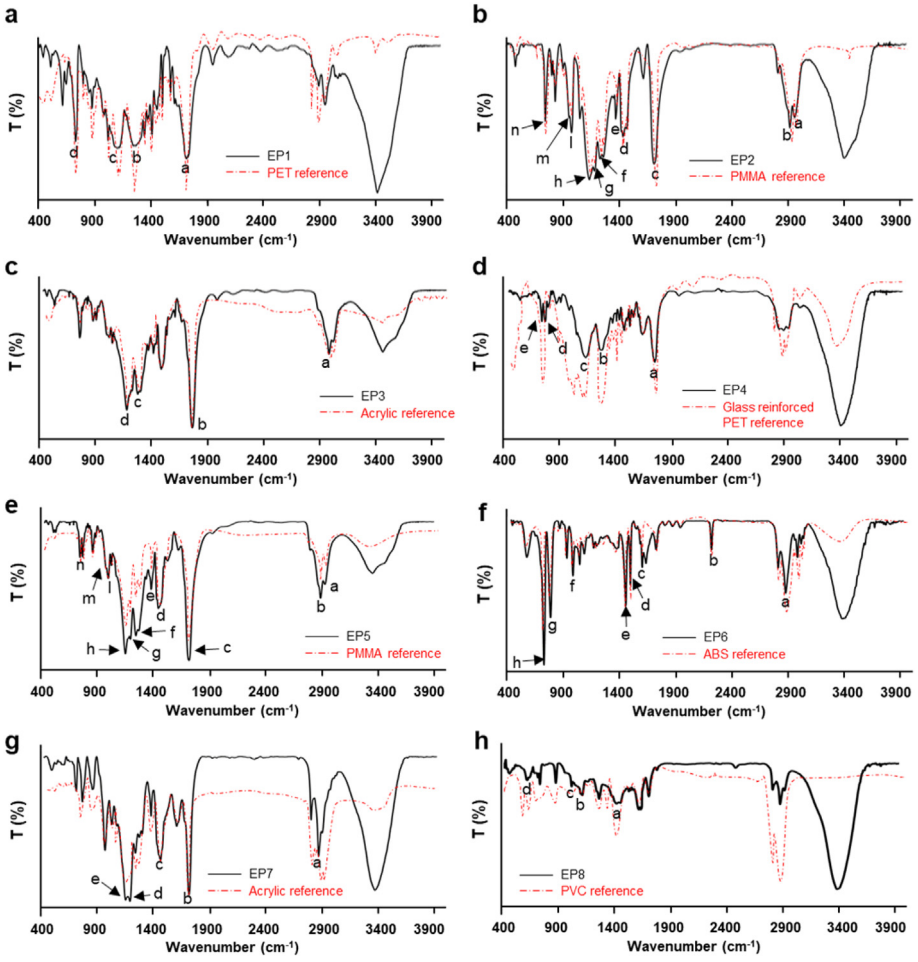

Fig. 1. FTIR spectra of all the E-plastics (black line) and the respective database matched spectra (red dash-dot line) for EP1 (a), EP2 (b), EP3 (c), EP4 (d), EP5 (e), EP6 (f), EP7 (g) and EP8 (h); the small alphabet labels in each FTIR spectrum indicate the respective characteristic absorption peaks of the samples. (For interpretation of the references to color in this figure legend, the reader is referred to the Web version of this article.)

Table 1
Characteristic bands and identifications of various E-plastics.

Sample ID	Identification by FTIR	Characteristics absorption bands (cm^{-1})	References
EP1	Polyethylene terephthalate (PET)	(a) 1713 C═O (b) 1241 C−O (c) 1094 C−O (d) 720 Aromatic CH (out-of-plane bend)	Jung et al. (2018)
EP2	Polymethyl methacrylate (PMMA)	(a) 2992 C−H (b) 2949 C−H (c) 1721 C═O (d) 1433 CH_2 (e) 1386 CH_3 (f) 1238 C−O (g) 1189 CH_3 (h) 1141 C−O (l) 985 CH_3 (m) 964 C−H (n) 750 C═O	Jung et al. (2018)
EP3	Acrylic and methacrylic polymers	(a) 2955 C−CH_3 (b) 1720 C═O (carbonyl group) (c) 1158 C−O−C (ether group) (d) 1253 C−O−C (epoxy group)	Dzulkurnain et al. (2015)
EP4	Glass polyethylene terephthalate (PET)	(a) 1713 C═O (b) 1241 C−O (c) 1094 C−O (d) 720 Aromatic CH (out-of-plane bend) (e) 700 Si−O−Si	Al-Oweini and El-Rassy (2009)
EP5	Polymethyl methacrylate (PMMA)	(a) 2992 C−H (b) 2949 C−H (c) 1721 C═O (d) 1433 CH_2 (e) 1386 CH_3 (f) 1238 C−O (g) 1189 CH_3 (h) 1141 C−O (l) 985 CH_3 (m) 964 C−H (n) 750 C═O	Jung et al. (2018)
EP6	Acrylonitrile butadiene styrene (ABS)	(a) 2922 C−H (b) 2238 C≡N (c) 1602 Aromatic ring (d) 1494 Aromatic ring (e)1452 CH2 (f) 966 = C−H (g) 759 Aromatic CH (h) 698 Aromatic CH	(Li et al., 2017; Jung et al., 2018)
EP7	Acrylic copolymers	(a) 2922 C−H (b) 1733 C═O (c) 1471 CH_2 & CH_3 (d) 1190 C−O (e) 1152 C−O−C	Al-Ali and Kassab-Bashi (2015)
EP8	Polyvinyl chloride (PVC)	(a) 1427 CH_2 (b) 1099 C−C (c) 966 CH_2 (d) 616 C−Cl	Jung et al. (2018)

detection limits in the tens of ppm (Oyedotun, 2018). Specific to the study, a handheld XRF analyzer was used to irradiate the samples with collimated X-ray beams (30 and 50 kV) of high intensity *in situ*. The elements detected in each E-plastic is compiled in Table 2. Our results revealed that the E-plastics contained a broad spectrum of toxic heavy metals such as copper (Cu), zinc (Zn), silver (Ag), barium (Ba), and antimony (Sb), etc. For each of the E-plastic samples, there is at least one toxic element that is present at levels higher than the permissible limits (#, Table 2) according to the RoHS and Directives of the European Parliament and the Council (2009/48/EC, 2011/65/EU, and 94/62/EC) standards. Remarkably, the highly toxic arsenic (As) was unexpectedly found to be present in EP1 (103.3 ppm) and EP8 (14.4 ppm), while lead (Pb) was detected in EP2 and EP6. Consistent with the FTIR analysis, a substantial amount of Cl (>200000 ppm) was detected in EP8 (PVC). It is also worth mentioning that the PVC contains arsenic (As) and a notable amount of antimony (Sb) as a synergist of halogen-based flame retardants.

3.3. TGA analysis

TGA was used to examine the thermal stability of E-plastics, as well as to quantify the filler contents, and their compositions. Shown in Fig. 2 are the TGA (green) and DTG (blue) graphs of EP1-

Table 2
Elemental analysis of E-plastics by XRF.

Sample ID	Elements (ppm)														
	Cl	Ca	Ti	Fe	Cu	Zn	As	Br	Sr	Ag	Sn	Sb	Ba	Pb	Bi
EP1	–	–	2.61×10^4	–	–	20.4	1.03×10^2	–	6.2×10^2	21.2	1.77×10	63	6.55×10^4	–	–
EP2	–	–	–	43	70.5	–	–	–	–	–	61.6	–	6.19×10^2	15.9	–
EP3	–	–	–	8.28×10^2	6.86×10^2	–	–	–	–	44.2	2.28×10^2	1.38×10^2	2.66×10^3	–	–
EP4	–	–	–	4.73×10^2	2.89×10^2	–	–	–	–	36.7	2.03×10^2	1.04×10^2	1.77×10^3	–	–
EP5	–	–	–	8.41×10^2	5.78×10^2	–	–	10.6	–	–	2.14×10^2	–	2.70×10^3	–	–
EP6	–	4.71×10^3	2.89×10^3	3.55×10^2	47	60.8	–	3.73×10^2	8.8	10.9	37.9	2.7×10^2	5.43×10^2	18	–
EP7	–	–	4.85×10^2	–	1.89×10^2	3.38×10^3	–	49.8	4.6	–	50.2	–	6.94×10^2	–	15
EP8	2.45×10^5	9.85×10^4	–	3.83×10^2	51.3	7.01×10^2	14.1	12.5	66.2	15.1	39.1	2.6×10^3	4.17×10^2	–	–

Cr, Mn, Co, Ni, Se, Zr, Mo, Cd, Au, and Hg are not detectable (–) in the E-plastics.
Permissible limits (restriction of hazardous substances, 2009/48/EC, 2011/65/EU, and 94/62/EC).
Cu (156 ppm); Zn (938 ppm); As (3.8 ppm); Sr (1125 ppm); Sn (3750 ppm); Sb (45 ppm); Ba (1125 ppm); Pb (13.5 ppm).
Highlighted figures denote element exceeds the safety limit.

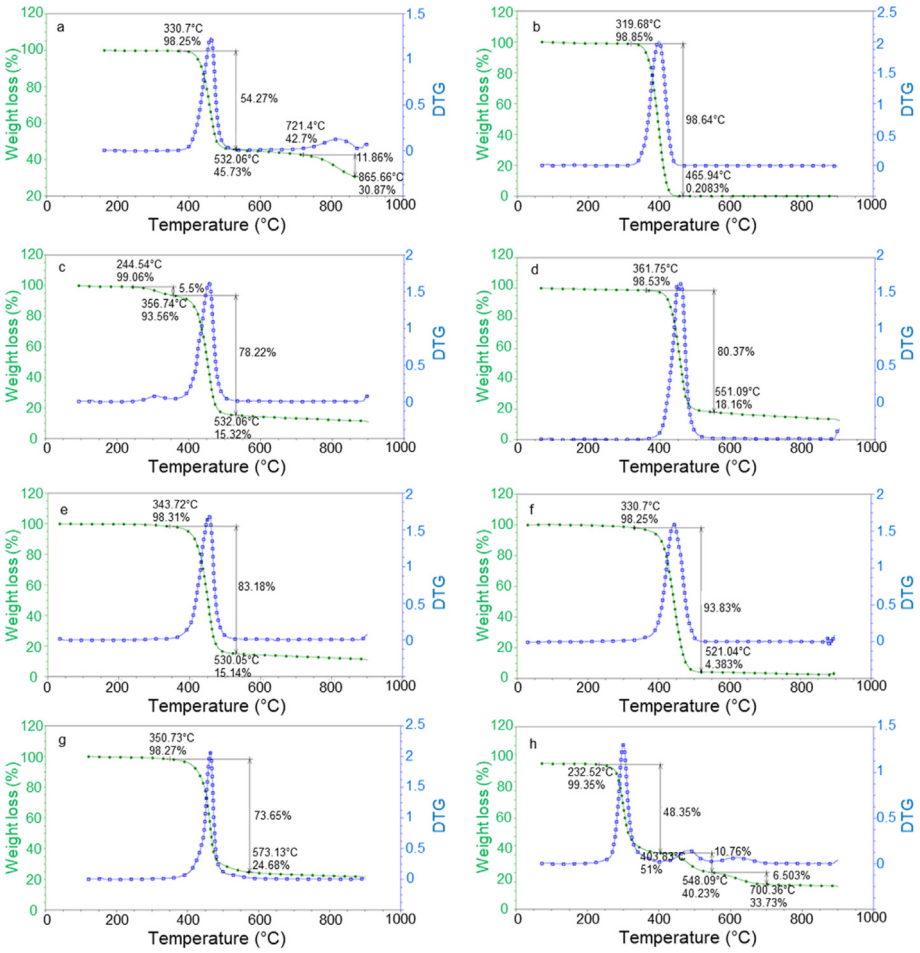

Fig. 2. Thermogravimetric analysis (TGA) of various E-plastics: EP1 (a), EP2 (b), EP3 (c), EP4 (d), EP5 (e), EP6 (f), EP7 (g) and EP8 (h); weight loss percentage: dot line (•); and Derivative weight loss vs Temperature: square line (□).

EP8. DTG illustrates the weight loss rate of plastics upon heating, and it is used here to simplify the readings of the starting and endpoints of E-plastic decomposition. All the E-plastics were found to be stable within the temperature range of 25–200 °C. At higher temperatures (250–900 °C), we observed a significant weight loss ranging from 65 to 99% across the different E-plastics, which corresponded to the burn-off (endothermic) of the respective polymer matrices. In the case of EP2 and EP6, the almost complete weight loss of the samples >500 °C suggests that the presence of mineral additives in the plastics are negligible. In stark contrast, varying amounts of non-decomposable residues (EP1: 28.76%, EP3: 5.75%, EP4: 13.13%, EP5: 11.72%, EP7: 22.24%, and EP8: 32.44%) were observed for the rest of the E-plastic samples. Based on the XRF analysis, it was postulated that Ti, Ba, and Zn compounds may be incorporated into the plastics as fillers (e.g. calcium carbonate), coloring additives (e.g. titanium dioxide, barium sulfate) and even mold lubricants (e.g. zinc stearate) (Liu et al., 2006; N.A.S. and Noreen, 2008; Subramanian, 2013). Of note is EP8 (PVC), which has a significant amount of residue of ~33% and contained the greatest number of metallic components among the representative E-plastics screened (Fig. 2 and Table 2). Calcium carbonate is typically incorporated in PVC to reduce abrasive wear, improve mechanical strength, and enhance protection against weathering (Liu et al., 2006; N.A.S. and Noreen, 2008).

3.4. Cytotoxicity assays

So far, our characterization data is consistent with existing literatures (Hahladakis et al., 2018; Turner, 2018), suggesting that the E-plastics contain numerous hazardous metal ions and additives. It has been reported that these harmful substances found in E-plastics may be released gradually in an aqueous environment, thereby rendering the plastics to be cytotoxic (Mao et al., 2020). Furthermore, the apoptosis-inducing potential of environmentally disintegrated microplastics was also recently documented in normal human embryonic kidney cell lines (HEK-293) (Sivagami et al., 2021). Conceivably, the amount of hazardous constituent and size of plastics has important bearings on the cytotoxic potential of waste plastics. Although it is possible to utilize plastic extracts to examine the toxicity of the polymer leachates (Zimmermann et al., 2019), the use of strong solvents during the extraction step is not representative of environmental exposures. Such unintended experimental bias may, therefore, skew the findings, leading to the over-interpretation of the toxic potential of plastic materials. Therefore, to decouple the “actual” and “apparent” cytotoxic potential of E-plastics, herein, cells were cultured in direct contact with the panel plastics for an extended period of time. Specifically, 6 different human cell lines were selected for our *in vitro* studies. The cells used in this study are HaCaT, HDF, MKN, SW480, MG63,

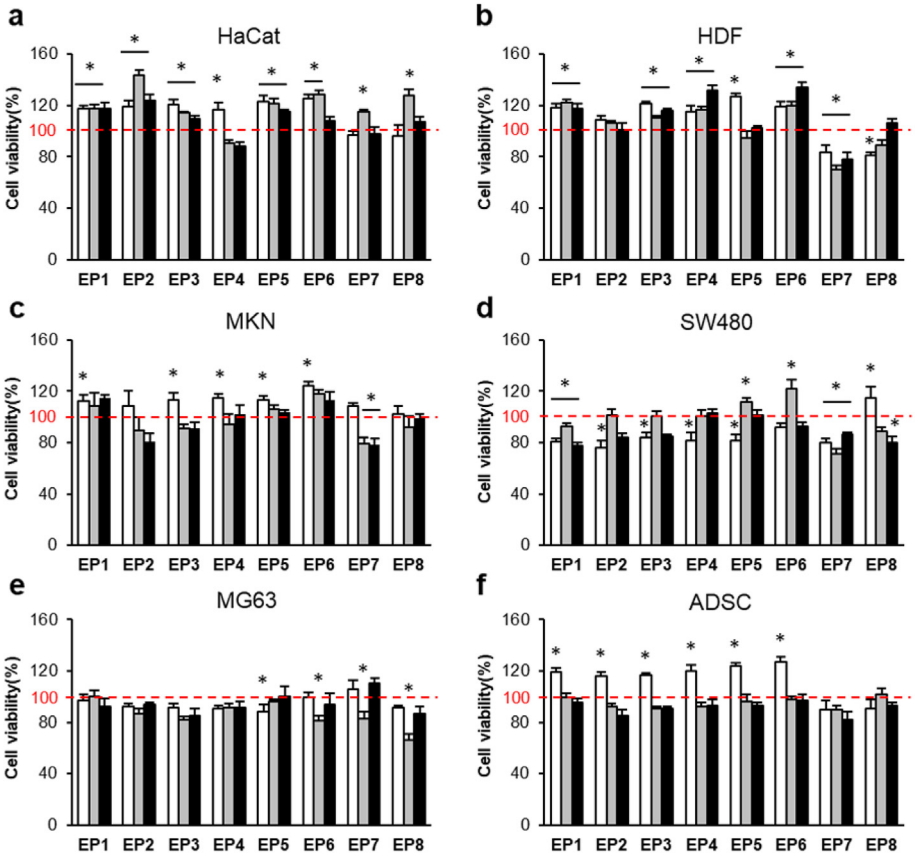

Fig. 3. Percentage cell viability of HaCaT (a), HDF (b), MKN (c), SW480 (d), MG63 (e) and ADSC (f) after 24 h (white bar), 96 h (gray bar) and 168 h (black bar) of culture on the respective E-plastics. Measured metabolic activities were normalized to recorded values obtained from cells grown on standard TCPs (red dashed line). All data are represented as mean ± standard deviation. Experiments were conducted in triplicates. * denotes statistical difference compared to the respective TCP control groups at $p < 0.05$. (For interpretation of the references to color in this figure legend, the reader is referred to the Web version of this article.)

and ADSCs. The time-dependent toxicity of the E-plastics was also evaluated at different time points (i.e. 24, 96, and 168 h), resulting in 144 unique E-plastic-cell type-exposure time permutations. To the best of our knowledge, this is by far the most comprehensive cytotoxicity study ever to be attempted on E-plastics.

Viabilities of the E-plastics exposed cells were measured using the PrestoBlue assay. The non-destructive nature of the assay, coupled with its excellent sensitivity, enables us to monitor the cell metabolism *in situ* over time. The computed percentage cell viability of the different cell types grown on the respective E-plastics is shown in Fig. 3. Cells grown on standard TCPs served as internal controls. Interestingly, we did not observe any significant toxicity for all the E-plastics that were screened. In general, the measured cell viabilities on the E-plastics were comparable to the control, with a normalized fluctuation of around ±20% across the different cell/E-plastics-time point permutations. Specifically, HaCaT (Fig. 3a) and HDF (Fig. 3b) consistently exhibited higher cell viability values on EP1-EP6 relative to the control. In the case of the other cell types (Fig. 3c–f), the cell viability values were not drastically different from their respective controls. These results strongly suggest that the biological response to the E-plastics is highly cell-specific, and some cells are more sensitive to the property of plastic surfaces. Furthermore, both EP7 and EP8 appear to have greater negative impacts on the cell viabilities for all cell types. Unlike EP1-6, HaCaT, and HDF cultured on EP7 and EP8 did not exhibit increased metabolic activities. Instead, we observed a slightly lowered HDF viability for the EP7 group at each exposure timepoint. Correspondingly, higher levels of Zn (3382.2 ppm) and Sb (2604 ppm) were also observed in EP7 and EP8 respectively (Table 2), which are easy>10-fold higher compared to the other E-plastics. This led us to postulate that the modest decrease in cell viability values may be attributed to the leaching of toxic ions from the source E-plastics. However, except for Sr, the leaching of metals detected in the cell culture medium was less than 1 ppb (Table S1). This strongly suggests that within our experimental timeframe, there is negligible outward diffusion of toxic metal ions in the biological milieu.

The slight decrease in cell viability for some cells as observed in Fig. 3 may not amount to an acute nor sub-chronic cytotoxic response, and the phenomena may be purely induced by the natural fluctuation of cell metabolic activity at each time point, as well as the ECM production process on the different plastic surface. To further confirm this postulation, we next employed live/dead staining with FDA and PI dyes. FDA is a cell-permeable esterase substrate that would rapidly hydrolyze into fluorescein in the cytoplasmic compartment of living cells to produce bright green fluorescence. Conversely, PI is an impermeable dye that is excluded in viable cells. A damaged cell membrane in a dead cell would allow PI to passage into the cell and intercalate with the nucleic acid to produce a bright red fluorescent signal. Therefore, the combined use of FDA and PI dyes would allow us to differentiate the viable (i.e. FDA (+)/PI (−)) and non-viable (i.e. FDA (−)/PI (+)) cells. The

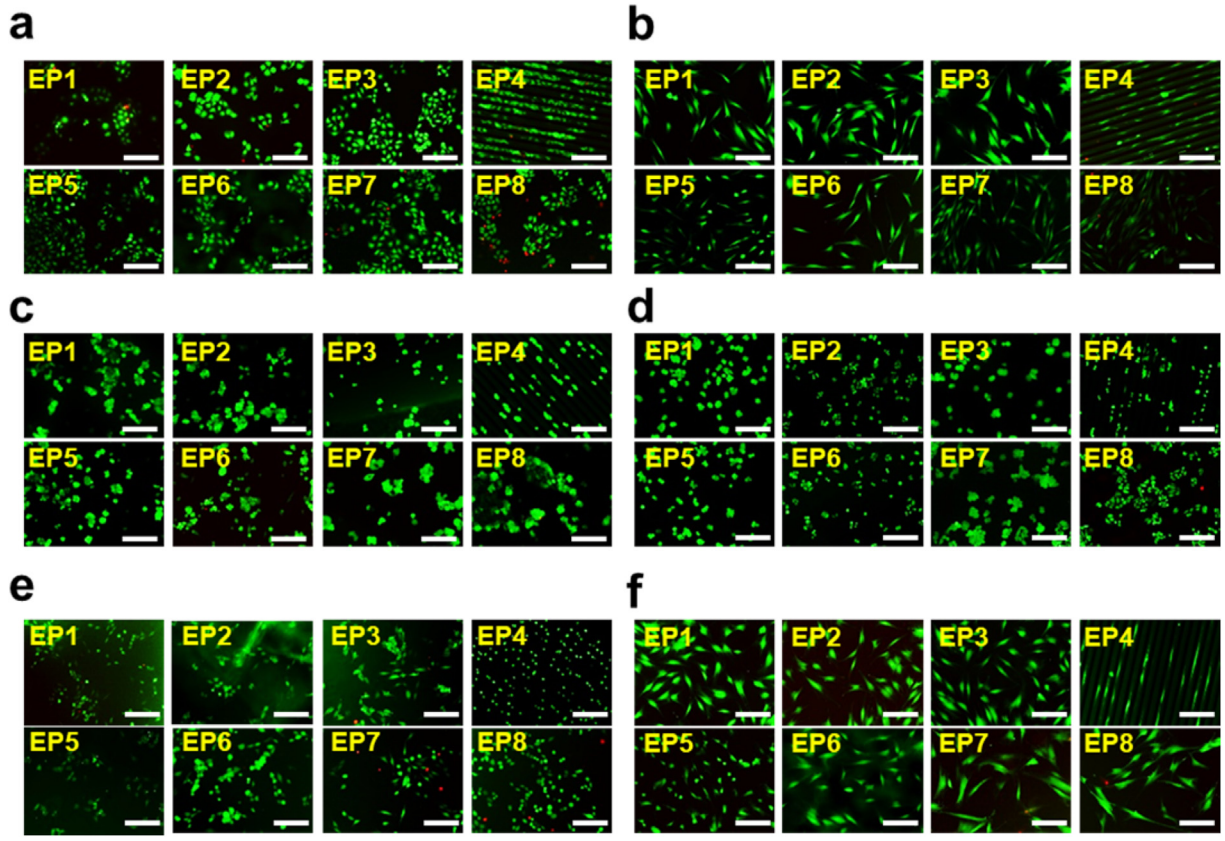

Fig. 4. Live (green)/dead (red) images of HaCaT (a), HDF (b), MKN (c), SW480 (d), MG63 (e) and ADSCs (f) on the various E-plastics after 24 h of culture. Scale bar: 200 μm. (For interpretation of the references to color in this figure legend, the reader is referred to the Web version of this article.)

representative FDA/PI staining images of the various cell lines on the E-plastics after 24 h of culture are shown in Fig. 4.

Consistent with the results obtained from the PrestoBlue assay, the metabolic activity of the cells grown on the E-plastics appears to be robust as indicated by the large number of FDA (+) cells. Conversely, the number of PI (+) cells are negligible, suggesting that the E-plastics are cytocompatible and support cell adhesion (Fig. S2). It is interesting to note that despite the known hydrophobic nature of the E-plastics, cells were still able to attach onto the plastic surface, albeit at varying degrees. Furthermore, the cells grown on EP4 were highly aligned at day 1 (Fig. 4), and the cell alignment was maintained at day 7 (Fig. 5). This could be attributed to the occurrence of micro-scale, angled ridges on its front-facing surface of the prism, which could guide cell attachment and migration via the process of "contact guidance" (Tay et al., 2011, 2013). As shown in Fig. 5, by day 7 (168 h) a significant increase in the number of FDA (+) cells were observed on all the E-plastic samples, while the occurrence of PI (+) cells remained negligible (Fig. S3). This implies that not only are the E-plastics non-toxic, but also able to support cell proliferation. Taken together, our results revealed that the E-plastics were stable under physiological conditions and that the leaching of the E-plastic bound toxic additives into the biological milieu (if any) was not sufficiently high to adversely affect cell viability within our experimental boundaries.

4. Conclusion

In this study, 8 representative discarded E-plastics from a local recycling plant were collected and analyzed. The E-plastics were thoroughly characterized using FTIR, TGA, and XRF. The E-plastics are composed mainly of PET, PMMA, acrylics, ABS, and PVC. Numerous hazardous heavy metals and halogen compounds were detected in all the E-plastics. A small library of 144 biological endpoints to examine the toxic potential of the E-plastics was generated. The overall toxicity of E-plastics depends heavily on the plastic types, cell types, and exposure time. Among the 6 human cell lines screened, HaCaT and HDF were observed to be more responsive to E-plastics exposure, whereas EP 7 and 8 exhibited greater perturbation to the cell metabolism. Nevertheless, follow-up examination using FDA and PI staining revealed that the cell viability of all cell lines remained high >90% despite being in close contact with the E-plastics over a period of 1 week. This can be explained by the negligible outward leaching of heavy metals from the plastic matrix. In the broader context, clarifying the innate toxic potential of the E-plastics in its pristine state is not only important from the public health perspective but also may open up new avenues for E-plastics to be upcycled for applications that may require the short term interaction with human cells. While the apparent cytotoxic potential of the screened E-plastics may be low, additional studies are warranted to examine in greater detail the

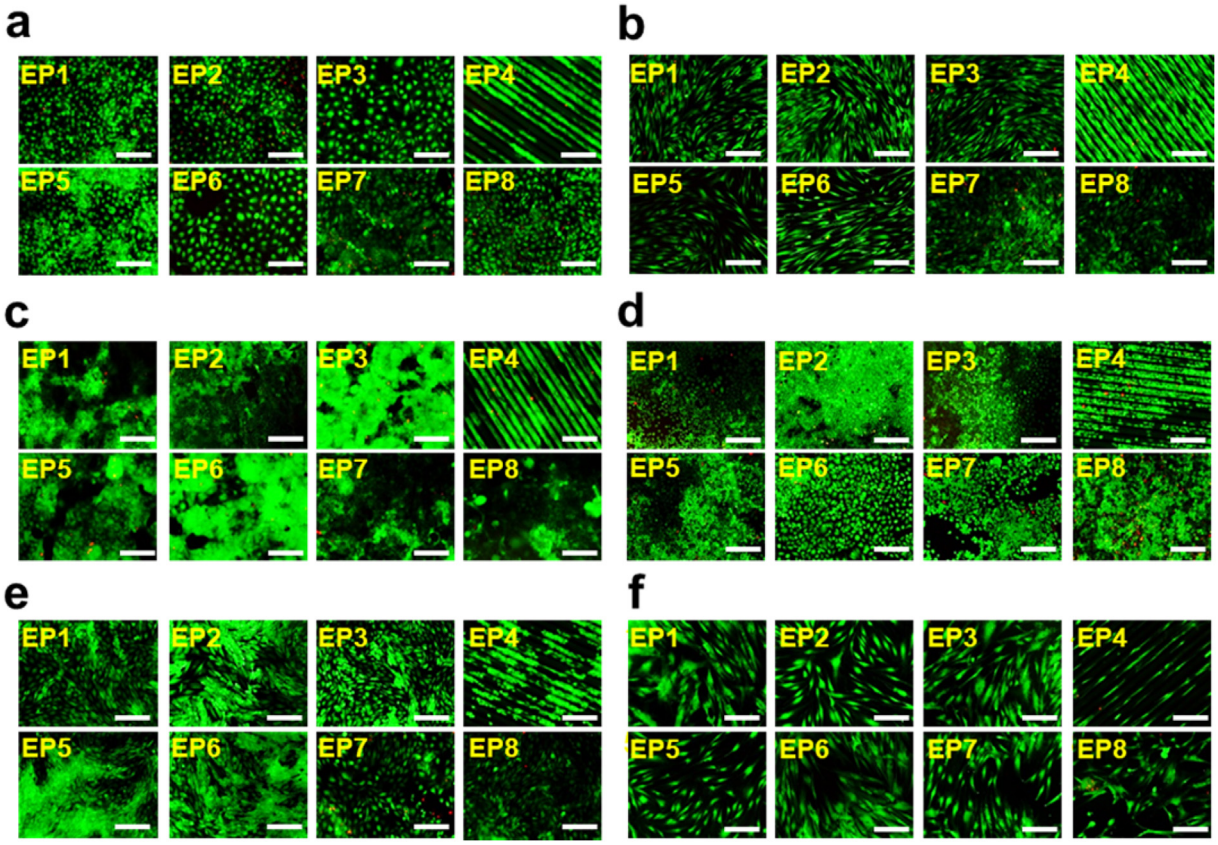

Fig. 5. Live (green)/dead (red) images of HaCaT (a), HDF (b), MKN (c), SW480 (d), MG63 (e) and ADSCs (f) on the various E-plastics after 168 h of culture. Scale bar: 200 μm. (For interpretation of the references to color in this figure legend, the reader is referred to the Web version of this article.)

toxicity of E-plastics in various operating environment along the entire E-waste CE value chain.

Credit author statement

Pujiang Shi, Methodology, Validation, Formal analysis, Investigation, Writing, Visualization. Yan Wan, Validation, Writing - review & editing. Agnès Grandjean, Writing - review & editing, Funding acquisition. Jong-Min Lee, Writing, Review, Editing, Funding acquisition. Chor Yong Tay, Conceptualization, Methodology, Investigation, Writing, Visualization, Supervision, Project administration, Funding acquisition

Declaration of competing interest

The authors declare that they have no known competing financial interests or personal relationships that could have appeared to influence the work reported in this paper.

Acknowledgment

This work was financially supported by a grant award from "Singapore –CEA Alliance for Research in Circular Economy (SCARCE)", which is a joint lab set up between Nanyang Technological University (NTU, Singapore) and the French Alternative Energies and Atomic Energy Commission (CEA, France). SCARCE is supported by the National Research Foundation, Prime Minister's Office, Singapore, the Ministry of National Development, Singapore, and National Environment Agency, Ministry of the Environment and Water Resource, Singapore under the Closing the Waste Loop R&D Initiative as part of the Urban Solutions & Sustainability – Integration Fund (award number USS-IF-2018-4). The authors also wish to thank Dr. Ange Anicet Maurice for assisting with the XRF characterization.

Appendix A. Supplementary data

Supplementary data to this article can be found online at https://doi.org/10.1016/j.chemosphere.2020.128719.

References

Al-Ali, A., Kassab-Bashi, T., 2015. Fourier transform infra red (FTIR) spectroscopy of new copolymers of acrylic resin denture base materials.
Al-Oweini, R., El-Rassy, H., 2009. Synthesis and characterization by FTIR spectroscopy of silica aerogels prepared using several Si(OR)4 and R′′Si(OR')3 precursors. J. Mol. Struct. 919, 140–145.
Ananda, S., Shaohua, Z., Liang, L., 2013. Fatal barium chloride poisoning: four cases report and literature review. Am. J. Forensic med. Patho 34, 115–118.
Branchi, I., Alleva, E., Costa, L.G., 2002. Effects of perinatal exposure to A polybrominated diphenyl ether (PBDE 99) on mouse neurobehavioural development. Neurotoxicology 23, 375–384.
Buekens, A., Yang, J., 2014. Recycling of WEEE plastics: a review. J. Mater. Cycles Waste Manag. 16, 415–434.
Cavallo, D., Iavicoli, I., Setini, A., Marinaccio, A., Perniconi, B., Carelli, G., Iavicoli, S., 2002. Genotoxic risk and oxidative DNA damage in workers exposed to antimony trioxide. Environ. Mol. Mutagen. 40, 184–189.
Chaqmaqchee, F.A.I., Baker, A.G., Salih, N.F., 2017. Comparison of various plastics wastes using X-ray fluorescence. Am J Mater Synth Process 5, 24–27.
Denys, S., Tack, K., Caboche, J., Delalain, P., 2009. Bioaccessibility, solid phase distribution, and speciation of Sb in soils and in digestive fluids. Chemosphere 74, 711–716.
Dufault, C., Poles, G., Driscoll, L.L., 2005. Brief postnatal PBDE exposure alters learning and the cholinergic modulation of attention in rats. Toxicol. Sci 88, 172–180.
Dzulkurnain, A., Hanifah, S., Ahmad, A., Mohamed, N.S., 2015. Characterization of

random methacrylate copolymers synthesized using free-radical bulk polymerization method. Int. J. Electrochem. Sci. 10, 84–92.
Eriksson, P., Jakobsson, E., Fredriksson, A., 2001. Brominated flame retardants: a novel class of developmental neurotoxicants in our environment? Environ. Health Perspect. 109, 903–908.
Hahladakis, J.N., Velis, C.A., Weber, R., Iacovidou, E., Purnell, P., 2018. An overview of chemical additives present in plastics: migration, release, fate and environmental impact during their use, disposal and recycling. J. Hazard Mater. 344, 179–199.
Hallgren, S., Darnerud, P.O., 2002. Polybrominated diphenyl ethers (PBDEs), polychlorinated biphenyls (PCBs) and chlorinated paraffins (CPs) in rats-testing interactions and mechanisms for thyroid hormone effects. Toxicology 177, 227–243.
Hamers, T., Kamstra, J.H., Sonneveld, E., Murk, A.J., Kester, M.H.A., Andersson, P.L., Legler, J., Brouwer, A., 2006. Vitro profiling of the endocrine-disrupting potency of brominated flame retardants. Toxicol. Sci 92, 157–173.
Jantsch, W., Kulig, K., Rumack, B.H., 1984. Massive copper sulfate ingestion resulting in hepatotoxicity. J. Toxicol. Clin. Toxicol. 22, 585–588.
Jung, M.R., Horgen, F.D., Orski, S.V., Rodriguez C, V., Beers, K.L., Balazs, G.H., Jones, T.T., Work, T.M., Brignac, K.C., Royer, S.-J., Hyrenbach, K.D., Jensen, B.A., Lynch, J.M., 2018. Validation of ATR FT-IR to identify polymers of plastic marine debris, including those ingested by marine organisms. Mar. Pollut. Bull. (Arch. Am. Art) 127, 704–716.
Li, J., Chen, F., Yang, L., Jiang, L., Dan, Y., 2017. FTIR analysis on aging characteristics of ABS/PC blend under UV-irradiation in air. Spectrochim. Acta 184, 361–367.
Liu, P., Zhao, M., Guo, J., 2006. Thermal stabilities of poly(vinyl chloride)/calcium carbonate (PVC/CaCO3). Composites. J Macromol Sci B 45, 1135–1140.
Ma, C., Yu, J., Wang, B., Song, Z., Xiang, J., Hu, S., Su, S., Sun, L., 2016. Chemical recycling of brominated flame retarded plastics from E-waste for clean fuels production: a review. Renew. Sust. Energy Rev. 61, 433–450.
Mao, S., Gu, W., Bai, J., Dong, B., Huang, Q., Zhao, J., Zhuang, X., Zhang, C., Yuan, W., Wang, J., 2020. Migration of heavy metal in electronic waste plastics during simulated recycling on A laboratory scale. Chemosphere 245, 125645.
Mishra, K.P., 2009. Lead exposure and its impact on immune system: a review. Toxicol. In. In Vitro 23, 969–972.
N A S, F., Noreen, T., 2008. The effect of precipitated calcium carbonate on the mechanical properties of poly(vinyl chloride).
Nnorom, I.C., Osibanjo, O., 2009. Toxicity characterization of waste mobile phone plastics. J. Hazard Mater. 161, 183–188.
Oyedotun, T.D.T., 2018. X-Ray fluorescence (XRF) in the investigation of the composition of earth materials: a review and an overview. Geology, Ecology, and Landscapes 2, 148–154.
Qiu, R., Lin, M., Qin, B., Xu, Z., Ruan, J., 2021. Environmental-friendly recovery of non-metallic resources from waste printed circuit boards: a review. J. Clean. Prod. 279, 123738.
Qiu, R., Lin, M., Ruan, J., Fu, Y., Hu, J., Deng, M., Tang, Y., Qiu, R., 2020. Recovering full metallic resources from waste printed circuit boards: a refined review. J. Clean. Prod. 244, 118690.
Rarotra, S., Sahu, S., Kumar, P., Kim, K.-H., Tsang, Y.F., Kumar, V., Kumar, P., Srinivasan, M., Veksha, A., Lisak, G., 2020. Progress and challenges on battery waste management :A critical review. Chemistry 5, 6182–6193.
Riise, B.L., Biddle, M.B., Fisher, M.M., 2000. X-ray fluorescence spectroscopy in plastic recycling. American plastics Council, APC/MBA polymer Project.
Sahajwalla, V., Gaikwad, V., 2018. The present and future of E-waste plastics recycling. Curr. Opin. Green Sustain. Chem. 13, 102–107.
Sarkar, A., Paul, B., 2016. The global menace of arsenic and its conventional remediation - a critical review. Chemosphere 158, 37–49.
Schlummer, M., Gruber, L., Mäurer, A., Wolz, G., van Eldik, R., 2007. Characterisation of polymer fractions from waste electrical and eectronic equipment (WEEE) and implications for waste management. Chemosphere 67, 1866–1876.
Senthil Kumar, K., Baskar, K., 2015. Recycling of E-plastic waste as A construction material in developing countries. J. Mater. Cycles Waste Manag. 17, 718–724.
Singh, N., Duan, H., Tang, Y., 2020. Toxicity evaluation of E-waste plastics and potential repercussions for human health. Environ. Bar Int. 137, 105559.
Sivagami, M., Selvambigai, M., Devan, U., Velangani, A.A.J., Karmegam, N., Biruntha, M., Arun, A., Kim, W., Govarthanan, M., Kumar, P., 2021. Extraction of microplastics from commonly used sea salts in India and their toxicological evaluation. Chemosphere 263, 128181.
Song, Q., Li, J., 2014. Environmental effects of heavy metals derived from the E-waste recycling activities in China: a systematic review. J. Waste manag, 34, 2587–2594.
Subramanian, M.N., 2013. Inorganic additives. In: Subramanian, M.N. (Ed.), Plastics Additives and Testing, pp. 125–144.
Tay, C.Y., Irvine, S.A., Boey, F.Y.C., Tan, L.P., Venkatraman, S., 2011. Micro-/Nano-engineered cellular responses for soft tissue engineering and biomedical applications. Small 7, 1361–1378.
Tay, C.Y., Koh, C.G., Tan, N.S., Leong, D.T., Tan, L.P., 2013. Mechanoregulation of stem cell fate via micro-/nano-scale manipulation for regenerative medicine. Nanomedicine 8, 623–638.
Turner, A., 2018. Black plastics: linear and circular economies, hazardous additives and marine pollution. Environ. Bar Int. 117, 308–318.
Vanessa Forti, C.P.B., Ruediger, Kuehr, Garam, Bel, 2020. The Global E-waste Monitor 2020 : quantities, flows, and the circular economy potential.
Vimala, J., Natesan, M., Rajendran, S., 2009. Corrosion and protection of electronic components in different environmental conditions - an overview. Open Corrosion J. 2, 105–113.
Wang, J.K., Cheam, N.M.J., Irvine, S.A., Tan, N.S., Venkatraman, S., Tay, C.Y., Interpenetrating network of alginate–human adipose extracellular matrix hydrogel for islet cells encapsulation. Macromolecular rapid communications n/a, 2000275.
Wani, A.L., Ara, A., Usmani, J.A., 2015. Lead toxicity: a review. Interdiscip. Toxicology 8, 55–64.
Weber, R., Kuch, B., 2003. Relevance of BFRs and thermal conditions on the formation pathways of brominated and brominated-chlorinated dibenzodioxins and dibenzofurans. Environ. Bar Int. 29, 699–710.
Wu, Z., Soh, T., Chan, J.J., Meng, S., Meyer, D., Srinivasan, M., Tay, C.Y., 2020. Repurposing of fruit peel waste as a green reductant for recycling of spent lithium-ion batteries. Environ. Sci. Technol. 54, 9681–9692.
Yan, T., Xiang, L., Xuejun, J., Chengzhi, C., Youbin, Q., Xuelan, Y., Yang, L., Changyan, P., Hui, C., 2012. Spatial learning and memory deficit of low level polybrominated diphenyl ethers-47 in male adult rat is modulated by intracellular glutamate receptors. J. Toxicol. Sci. 37, 223–233.
Zimmermann, L., Dierkes, G., Ternes, T.A., Völker, C., Wagner, M., 2019. Benchmarking the in vitro toxicity and chemical composition of plastic consumer products. Environ. Sci. Technol. 53, 11467–11477.